

﴿ بِسْمِ اللَّهِ الرَّحْمَنِ الرَّحِيمِ ﴾

قَالُوا سُبْحَانَكَ لَا عِلْمَ لَنَا إِلَّا مَا عَلَّمْتَنَا إِنَّكَ أَنْتَ الْعَلِيمُ الْحَكِيمُ

صدق الله العظيم

دور الطرق التصويرية الحديثة في تشخيص وعلاج أورام الكلى السرطانية

رسالة مقدمة من

الطبيب / عمرو صلاح الدين أحمد نبيه النبال

بكالوريوس الطب والجراحة

جامعة القاهرة

توطئة للحصول على درجة الماجستير في الأشعة التشخيصية

المشرفون

أ. أشرف سعد زغلول

أستاذ مساعد جراحة الأورام

معهد الأورام القومي – جامعة القاهرة

أ.إ.آ. سامح عبد العزيز حنا

أستاذ الأشعة التشخيصية

كلية الطب – جامعة القاهرة

أ. أمل رفعت سيد

أستاذ مساعد الأشعة التشخيصية

معهد الأورام القومي – جامعة القاهرة

جامعة القاهرة

2008

ROLE OF NEW IMAGING MODALITIES IN MANAGEMENT OF MALIGNANT RENAL TUMORS

ESSAY

**Submitted For Partial Fulfillment of the M.Sc. degree in
Radiodiagnosis**

By

Amr Salah Eldin Ahmed Nabih ElNayal

M.B., B.CH.

Cairo University

Supervisors

Prof. Dr. Sameh Abdel Aziz Hanna

Professor of Radiodiagnosis
Faculty of Medicine
Cairo University

Dr. Ashraf Saad Zaghloul

Assist. Professor of Surgical oncology
National Cancer Institute
Cairo University

Dr. Amal Refaat Sayed

Assist. Professor of Radiodiagnosis
National Cancer Institute
Cairo University

Cairo University

2008

Abstract

Multiple imaging modalities are now used for assessment and management of renal masses. Ultrasound continues to play its initial role in diagnosis and characterization of renal masses, this role is further emphasized by contrast enhanced Ultrasound. Refinements in techniques of Multislice CT and MRI continue to improve image quality and detectability of renal masses along with the introduction of Positron emission tomography. Radiofrequency and Cryo-ablation are now considered as acceptable therapeutic options.

Key words :-

Renal – malignant– Multislice- Radiofrequency-Cryoablation

List of Abbreviations

- § 1 T : One Tesla
- § 1D : One dimensional
- § 2D: two dimensional
- § 3D : Three Dimensional
- § ACR: American College of Radiology
- § ADC: Apparent Diffusion Coefficient
- § AML: Angiomyolipoma
- § b.i.d : bis in die (twice/day)
- § BFGF: Basic fibroblast growth factor
- § CEUS: Contrast enhanced Ultrasonography
- § CLL: Chronic Lymphatic Leukemia
- § CMP: Cortico-medullary phase
- § CP: Cortical phase
- § CPR : Curved Planar reconstruction
- § CPS: Contrast Pulse Sequencing
- § CT : Computed Tomography
- § CTA : Computed Tomographic Angiography
- § CTU : Compute Tomographic Urography
- § DMSA: Dimercapto-Succinic acid
- § EP: Excretory phase
- § F: French (size unit of catheters)
- § FDG: Fluoro-deoxy-glucose
- § G : Gauge
- § GRE : Gradient echo
- § HASTE : Half Fourier acquisition single shot turbo spin echo
- § HU : Hounsfield unit
- § INV: Invasive
- § IP: In Progress
- § IVC: Inferior Vena Cava
- § IVU: Intravenous Urography
- § mA : Milli-amperes
- § MBq: Mega Becquerel
- § MDCT: Multidetector computed Tomography
- § MHz: Mega Hertz
- § MI : Mechanical index
- § MIP: Maximum intensity Projection
- § MPR : Multiplanar Reconstruction
- § MRA: Magnetic Resonance Angiography
- § MRI: Magnetic Resonance Imaging

§ MRU : Magnetic Resonance Urography
§ MRV: Magnetic Resonance Venography
§ NP: Nephrographic phase
§ NSS: Nephron sparing surgery
§ Nuc: Nuclear
§ P: P Value
§ PCS: Pelvicalyceal system
§ PDGF: Platelet derived growth factor
§ PET: Positron Emission Tomography
§ PRF: Pulse repetition frequency
§ PVA: Polyvinyl Alcohol
§ RBCS: Red blood cells
§ RCC: Renal cell carcinoma
§ RF : Radiofrequency
§ RFA: Radiofrequency Ablation
§ RRL: Relative Radiation Level
§ SENSE: Sensitivity encoding for Fast MRI
§ SMA : Superior mesenteric artery
§ SNR : Signal to Noise Ratio
§ SPECT: single photon emission Computed Tomography
§ SSR: Surface shaded Display
§ TAE : Transarterial Embolization
§ TCC: Transitional cell carcinoma
§ TE : Time of Echo
§ TR: Time of Recovery
§ US: Ultrasound
§ USCA(s): Ultrasound contrast agents
§ USPIO : Ultra-small super paramagnetic iron oxide particles
§ VEGF: vascular endothelial growth factor
§ VR : Volume rendered
§ VRI: Vascular Recognition Imaging
§ vs. :Versus

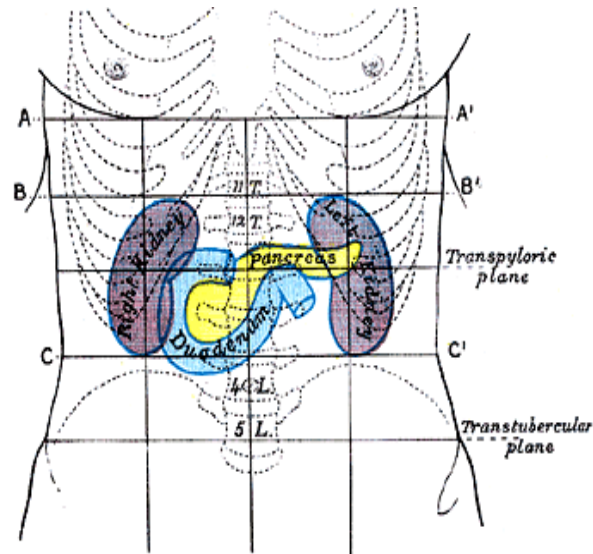
List of figures

Fig.1	P.5'	Fig.31	P.27'	Fig.61	P.54'	Fig.91	P.93'
Fig.2	P.5'	Fig.32	P.27'	Fig.62	P.55'	Fig.92	P.93'
Fig.3	P.6'	Fig.33	P.30'	Fig.63	P.56'	Fig.93	P.95'
Fig.4	P.6'	Fig.34	P.30'	Fig.64	P.56'	Fig.94	P.99'
Fig.5	P.9'	Fig.35	P.31'	Fig.65	P.57'	Fig.95	P.101'
Fig.6	P.9'	Fig.36	P.31'	Fig.66	P.57'	Fig.96	P.106'
Fig.7	P.10'	Fig.37	P.36',37'	Fig.67	P.58'	Fig.97	P.106'
Fig.8	P.11'	Fig.38	P.42'	Fig.68	P.58'	Fig.98	P.106'
Fig.9	P.12'	Fig.39	P.42'	Fig.69	P.63'	Fig.99	P.109'
Fig.10	P.12'	Fig.40	P.43'	Fig.70	P.63'	Fig.100	P.109'
Fig.11	P.13'	Fig.41	P.43'	Fig.71	P.65'	Fig.101	P.110'
Fig.12	P.14'	Fig.42	P.45'	Fig.72	P.65'	Fig.102	P.111',112'
Fig.13	P.15'	Fig.43	P.45'	Fig.73	P.69'		
Fig.14	P.16'	Fig.44	P.46'	Fig.74	P.69'		
Fig.15	P.16'	Fig.45	P.46'	Fig.75	P.71'		
Fig.16	P.16	Fig.46	P.46'	Fig.76	P.72'		
Fig.17	P.18'	Fig.47	P.47'	Fig.77	P.73'		
Fig.18	P.19'	Fig.48	P.47'	Fig.78	P.74'		
Fig.19	P.19'	Fig.49	P.48'	Fig.79	P.75'		
Fig.20	P.20'	Fig.50	P.48'	Fig.80	P.76'		
Fig.21	P.20'	Fig.51	P.49'	Fig.81	P.77'		
Fig.22	P.21'	Fig.52	P.50'	Fig.82	P.80'		
Fig.23	P.21'	Fig.53	P.50'	Fig.83	P.80'		
Fig.24	P.22'	Fig.54	P.51'	Fig.84	P.81'		
Fig.25	P.23'	Fig.55	P.52'	Fig.85	P.81'		
Fig.26	P.24'	Fig.56	P.52'	Fig.86	P.86'		
Fig.27	P.24'	Fig.57	P.52'	Fig.87	P.89'		
Fig.28	P.25'	Fig.58	P.53'	Fig.88	P.90'		
Fig.29	P.25'	Fig.59	P.53'	Fig.89	P.91'		
Fig.30	P.25	Fig.60	P.54'	Fig.90	P.92'		

List of Tables

No.	Title	Page
1	Robson system of classification of RCC	17
2	TNM staging of renal cell carcinoma	18
3	Pediatric Renal tumors	19
4	Staging of Wilms tumor	21
5	Grading of Transitional cell carcinoma	22
6	Classification of cystic renal lesions	45
7	Biopsy Results Categorized by Needle Type and Gauge	82
8	Comparison of ablative techniques with LPN	96
9	Radiofrequency ablation series	97
10	Cryoablation series	103

Introduction



(Fig.1) Front of abdomen, showing surface markings for duodenum, pancreas, and kidneys. AA; plane through point between body and xiphoid process of sternum. BB; plane midway bet. AA, and transpyloric plan. CC; plane midway between transpyoric and transtubercular planes (*Quoted from Williams et al , 1995*).

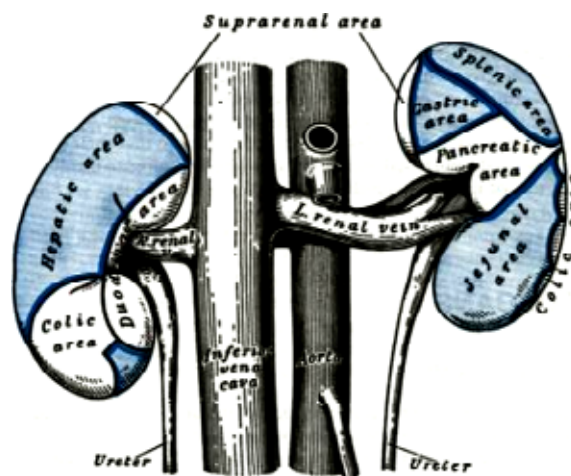


(Fig.2) The anterior surfaces of the kidneys, showing areas related to neighboring viscera (*Quoted from Williams et al , 1995*).

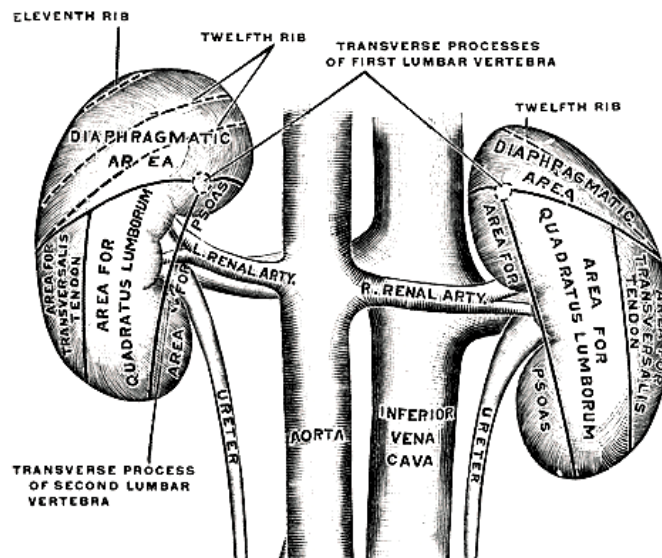


(Fig.3) The posterior surfaces of the kidneys, showing areas related to the posterior abdominal wall (*Quoted from Williams et al, 1995*).

(Fig.4) Longitudinal section through a kidney showing renal cortex, medulla, and pelvis. Renal pelvis has been opened to expose the hilum of the kidney (*Quoted from Sobotta, 1997*).

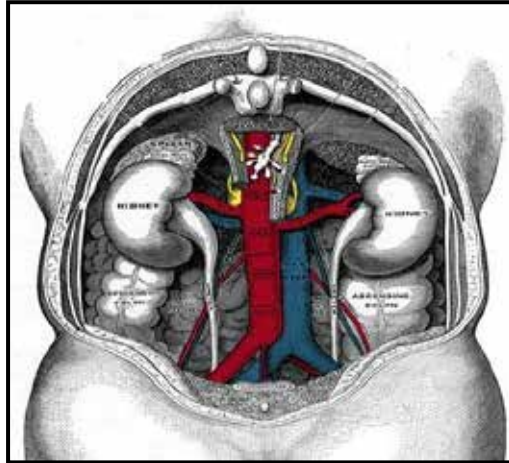


(Fig.5) Diagram illustrating the blood supply of the kidneys and ureters (*Quoted from Chummy, 1999*).

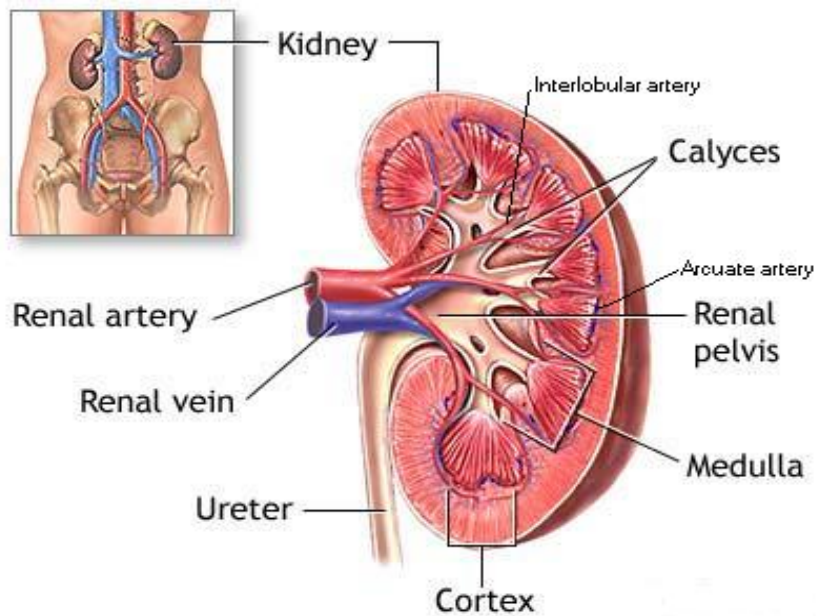


(Fig.6) Diagram illustrating renal structure, blood supply of the kidneys and ureters (*Quoted from Chummy, 1999*).

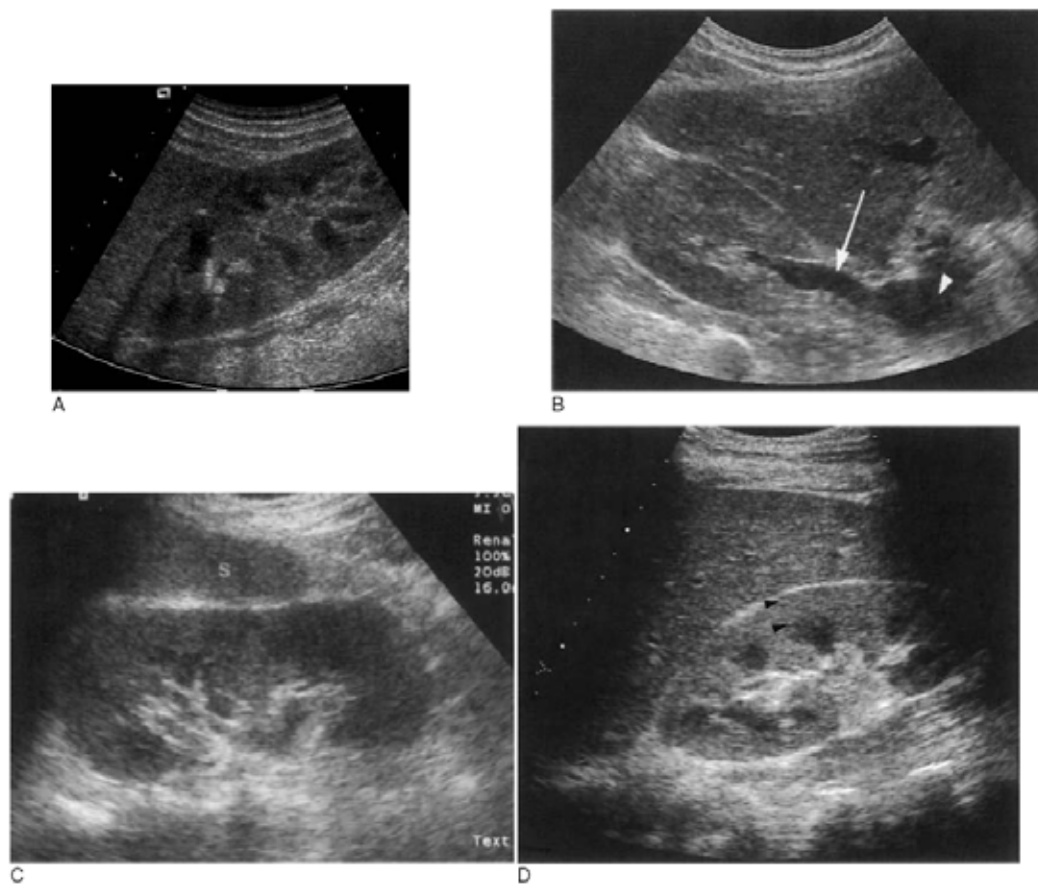


(Fig.7) (A) Sagittal section through the normal right kidney (RK), using the liver as an acoustic window. The central echoes from the renal sinus are hyperechoic due to the fat content. The hypoechoic, triangular, medullary pyramids are demonstrated in a regular arrangement around the sinus. The cortex is of similar echogenicity to the liver. (B) TS through the hilum of the RK, demonstrating the renal vein (arrow) draining into the inferior vena cava (IVC) (arrowhead). (C) Left kidney (LK) in coronal section. The renal hilum is seen furthest from the transducer (s = spleen). (Compare this with the *sagittal* section of the RK in which cortex is seen all the way around the pelvicalyceal system.) (D) The renal cortex lies between the capsule and the lateral margin of the medullary pyramid (arrowheads) *(Quoted from Bates, 2004).*

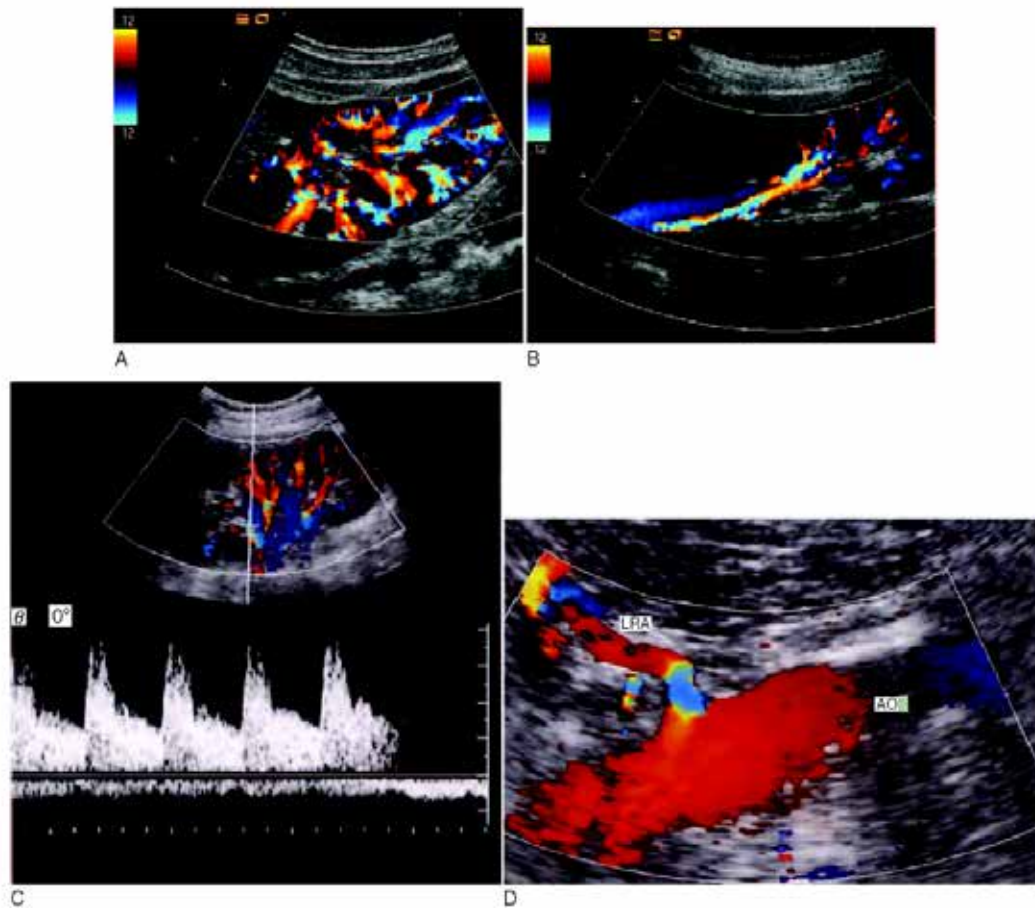


(Fig.8) (A) Color Doppler of the RK in coronal section demonstrates normal global intrarenal perfusion throughout the kidney. (B) TS through the LK demonstrates the main renal vein (blue) draining into the IVC. The main renal artery can be seen in red alongside. (C) The waveform from the main renal artery at the hilum of the kidney is of low resistance with good end-diastolic flow. The spectrum from the adjacent vein can be seen below the baseline. (D) Coronal section through the aorta (AO) showing the origin of the left renal artery. The blue colour in the proximal section of the artery is an aliasing artifact due to the strong Doppler signal from this part of the vessel, which is parallel to the beam. (Compare this with the aorta, which, because of its relatively perpendicular angle with the beam, has a poor Doppler signal, despite its high velocity in reality (*Quoted from Bates, 2004*).

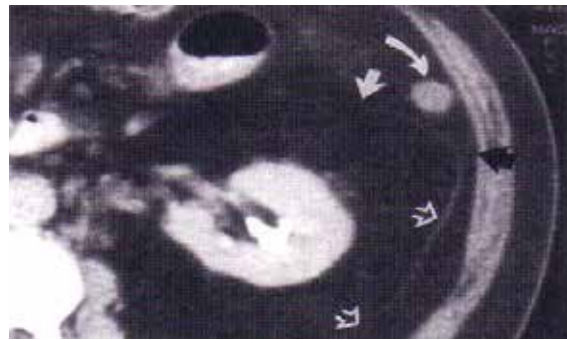


(Fig.9) Axial CT shows the posterior renal fascia (*open arrows*) separates the perinephric and posterior pararenal spaces. The anterior renal fascia (*straight white arrow*) separates the perinephric and anterior pararenal spaces. The lateroconal fascia (*black arrow*) extends lateral to the descending colon (*curved arrow*) (*Quoted from Haaga et al, 2003*).

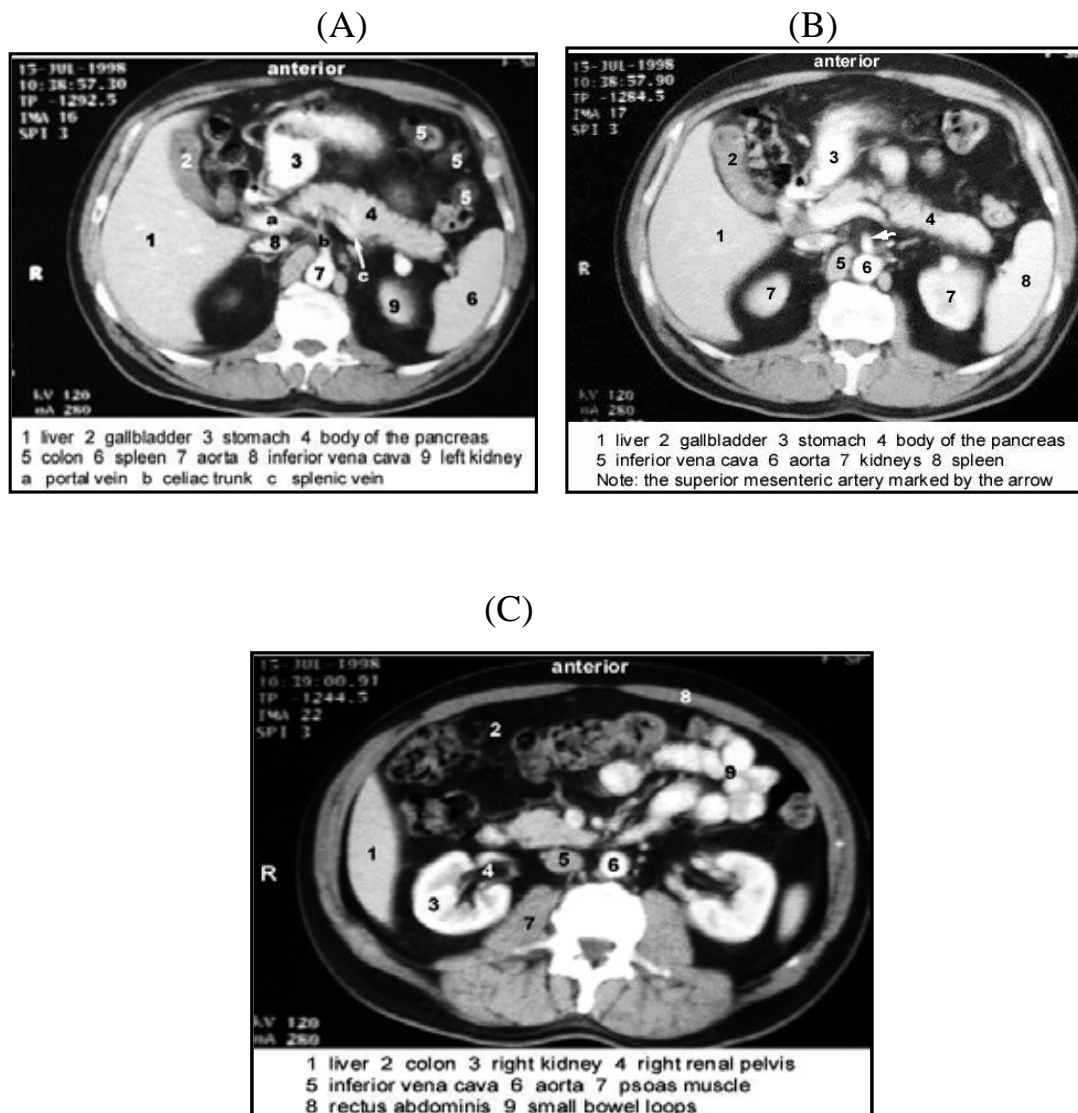


(Fig.10) Contrast enhanced helical CT sections showing both kidneys and their relations to the surrounding structures (*Quoted from Torsten and Emil, 1994*).